

RESEARCH

Open Access



# Extracellular vesicle miRNAs for predicting the efficacy of late-line treatment with anlotinib in patients with lung adenocarcinoma

Aimi Huang<sup>1†</sup>, Fuchuang Zhang<sup>2†</sup>, Jiyang Zhang<sup>2†</sup>, Xiaoya Xu<sup>2</sup>, Zhikuan Li<sup>2</sup>, Sheng Chen<sup>2</sup>, Baoning Nian<sup>2</sup>, Dadong Zhang<sup>2\*</sup>, Baohui Han<sup>1\*</sup>, Aiqin Gu<sup>1\*</sup> and Weimin Wang<sup>1\*</sup>

<sup>†</sup>Aimi Huang, Fuchuang Zhang and Jiyang Zhang have contributed equally to this work and share first authorship.

\*Correspondence: dadong.zhang@3dmedcare.com; hanxkyy@aliyun.com; guaiqin11@126.com; 13817680693@139.com

<sup>1</sup> Department of Pulmonary and Critical Care Medicine, Shanghai Chest Hospital, Shanghai Jiao Tong University, 241 Huaihai Road, Shanghai 200090, China  
<sup>2</sup> Department of Clinical and Translational Medicine, 3D Medicines Inc., Shanghai 201114, China

## Abstract

**Background:** Anlotinib is a targeted therapy indicated for some malignancies, including advanced non-small cell lung cancer (NSCLC). However, noninvasive biomarkers for identifying patients who will benefit from this disease remain lacking.

**Methods:** Here, we investigated the potential of small extracellular vesicle (sEV) microRNAs (miRNAs) as predictive biomarkers for anlotinib efficacy. A total of 20 advanced NSCLC patients were enrolled. Patients were classified as having stable disease (SD) or progressive disease (PD) after the initial efficacy assessment.

**Results:** Seven differentially expressed miRNAs (DEMs) were identified. Among them, miR-941 was significantly upregulated in the PD group, while the others were downregulated. Furthermore, these six downregulated miRNAs (miR-30a-3p, miR-150-5p, miR-122-5p, miR-10b-5p, miR-92a-3p, and miR-150-3p) were more pronounced in non-smoking patients.

**Conclusions:** It was found that sEV miRNAs have the potential to predict the benefit of anlotinib.

**Keywords:** sEVs, miRNA, Anlotinib, NSCLC

## Background

Anlotinib is a new small-molecule multitarget tyrosine kinase inhibitor (TKI) that has been approved for treating advanced NSCLC (Shen et al. 2018). In several clinical trials, anlotinib has shown good efficacy, safety, and significant advantages in treating advanced NSCLC (Zhang et al. 2020). Anlotinib has become an important third-line treatment option for advanced NSCLC and has been included in the recommendations of many national and international guidelines (Zhu et al. 2023). Anlotinib treatment prolongs patients' lives, improves quality of life, reduces symptoms, and improves prognosis (Kong et al. 2023). However, effective biological markers for evaluating the efficacy of anlotinib in treating advanced NSCLC remain lacking.



As a novel type of liquid biopsy technology, EVs have substantial potential in the field of tumor diagnosis (Li et al. 2023a). EVs are derived from various cells in the body, are rich in biologically active substances, and can reliably reflect the status of the parent cells, thus providing valuable biological information (Zhang et al. 2023b). An increasing number of studies have shown that EVs can be used as tumor markers for diagnosis, disease assessment, and prognosis determination (Guo et al. 2021; Li et al. 2021; Zheng et al. 2022). EVs can be found in blood, urine, and other body fluids and can be collected and detected in a noninvasive manner, which is important for the early diagnosis of tumors. sEV miRNAs, which are highly stable and specific and can reflect the biological status and function of tumor cells, have been reported to have potential in the assessment of tumor prognosis and in the monitoring of treatment in many cancers, such as ovarian (Li et al. 2023a, 2021), lung (Zheng et al. 2022), and pancreatic (Guo et al. 2021) cancer. However, it is unclear whether sEV miRNAs have a predictive role in the outcomes of treating advanced NSCLC patients with anlotinib.

In this study, small RNA sequencing was used to assess the expression levels of plasma sEV miRNAs in NSCLC patients with SD and PD. After integration analysis, we identified seven sEV miRNAs that were DEMs between SD and PD. Among them, miR-941 expression was upregulated in the PD group. However, the expression of miR-30a-3p, miR-150-5p, miR-122-5p, miR-10b-5p, miR-92a-3p, and miR-150-3p was significantly downregulated in the PD group. The signaling pathways associated with these DEMs were further analyzed. Our results suggest that sEV miRNAs may be novel predictive biomarkers for selecting patients who will benefit from anlotinib.

## Materials and methods

### Patient and study approval

The patients enrolled in this study were evaluated according to computed tomography (CT) examination results obtained 6 weeks after the initial administration of anlotinib. The classification criteria for SD and PD were based on the RECIST 1.1 assessment. A patient is classified as having SD if the tumor has shrunk by <30% and increased by <20%, with no new lesions. PD is defined as an increase in the maximum diameter of the tumor by >20% or the appearance of new lesions.

Blood samples were collected at Shanghai Chest Hospital, Shanghai Jiao Tong University School of Medicine. This study was approved by the Ethics Committee of Shanghai Chest Hospital (IS22010) and was registered on ClinicalTrials.gov (<https://clinicaltrials.gov/>) under the registration number NCT05218759. All participants in this study provided informed medical consent (Additional file 1: Table S1). Analyses and experiments involving human blood samples were performed in accordance with the tenets of the Declaration of Helsinki and Good Clinical Practice and in compliance with applicable regulations.

### sEV isolation

sEV isolation methods have been reported previously (Li et al. 2023a). Briefly, plasma samples were centrifuged (12,000 × g, 4 °C, 10 min) after incubation in a water bath at 37 °C for 5 min. The collected supernatants were filtered through 0.45 μm filters. Following centrifugation (12,000 × g, 4 °C, 5 min), the samples were filtered through 0.22 μm

tubular filters. After centrifugation ( $12,000 \times g$ ,  $4^\circ\text{C}$ , 5 min), the supernatant was collected and transferred to new tubes. A 25% volume of sEV isolation reagent (L3525; 3DMed, Shanghai) was added to the supernatant. After careful mixing and incubation at  $4^\circ\text{C}$  for 30 min, the samples were centrifuged at  $4700 \times g$  for 30 min at  $4^\circ\text{C}$ . The resulting pellet containing the sEVs was resuspended in PBS.

#### **Nanoparticle tracking analysis (NTA)**

A NanoSight NS 300 system (NanoSight Technology, Malvern) was used to characterize and track the size and number of sEVs. sEVs were resuspended at a concentration of  $5 \mu\text{g}/\text{mL}$  in PBS. The final concentration of sEVs was diluted to achieve 20–100 objects per frame. The sEV samples were placed in sample chambers and irradiated with a 488 nm laser using a scientific complementary metal oxide camera. NTA analytical software (version 2.3) was used to analyze the nanoparticle tracking data.

#### **Transmission electron microscopy (TEM)**

The sEV samples were resuspended in PBS and fixed with a 4% paraformaldehyde solution. The sEVs were then transferred to carbon-coated electron microscopy grids. After two rinses with PBS, the sEV samples were washed with glycine-containing PBS and then treated with 0.5% BSA in PBS for 10 min. The sEVs were then stained with 2% uranyl acetate, and a Hitachi H-7650 transmission electron microscope was used for examination and image collection.

#### **Nanoview analysis**

ExoView Tetraspanin Chips were used to identify plasma sEVs. Antibodies against CD63 (Alexa 647), CD81 (Alexa 555), and CD9 (Alexa 488) were generated and incubated with sEVs on the chips for 16 h. The chips containing sEVs were then washed with PBS containing Tween (PBST) and PBS. After washing, antibody colocalization analysis was performed using ExoView Tetraspanin kits. Plasma sEVs were then imaged and characterized using an ExoView R100 scanner. NanoViewer software was used to analyze the results further.

#### **Small RNA library preparation and sequencing**

RNA isolation from sEVs was performed using the silica gel membrane adsorption column method (217184, QIAGEN, Shanghai, China), which included sEV cleavage, extraction, incubation, centrifugation, enrichment of sEV RNA by an adsorption column, and washing 3 times. Finally, sEV RNA was obtained by elution with  $15 \mu\text{l}$  of enzyme-free water. We used an Agilent Small RNA Kit (5067–1548, Agilent, USA) to determine the quality of the sEV RNA. Total RNA was greater than 0.55 ng (concentration greater than  $36.7 \text{ pg}/\mu\text{l}$ ), and the proportion of miRNA was greater than 20%, which was sufficient for small RNA library construction. A total of  $6 \mu\text{l}$  of RNA per sample was used for miRNA library construction following the manufacturer's guidelines using the NEBNext Multiplexed Illumina RNA Isolation Kit (E7300L, NEB, USA). Briefly, the library was generated by ligation of the 3' adaptor, hybridization with reverse transcription primers, ligation of the 5' adaptor, reverse transcription, and PCR amplification. A NucleoSpin Gel and PCR Clean-up Kit (MACHEREY–NAGEL, Germany) was then used to purify

the DNA libraries. Library quality and distribution were assessed using an Agilent 2100 Bioanalyzer and a Highly Sensitive DNA Kit (5067–4626, Agilent, USA). The libraries were sequenced on an Illumina NovaSeq 6000 analyzer. The supplementary quality control results for the libraries are presented in Additional file 1, which includes Figures S1, S2 for visual data representation, as well as Tables S2, S3 for detailed numerical data. The library sizes ranged from 140 to 150 base pairs. After adapter clipping and quality filtering, the sequencing reads were aligned and mapped to the human genome. The input read count for each sample ranged from 18.5 to 104.9 million reads. Most of the samples achieved an alignment rate of more than 95% to the human genome. Additionally, the mapping rates for protein-coding genes, introns, long intergenic noncoding RNAs (lincRNAs), ribosomal RNAs (rRNAs), and miRNAs are detailed in Additional file 2: Table S4.

#### **Bioinformatics analysis of small RNA sequencing data**

Cutadapt (<https://doi.org/10.14806/ej.17.1.200>) was used to trim the 3' adapters for small RNA sequencing. After trimming, all the retained reads were aligned to the human genome (GRCh37) and annotated using Gencode (version 25) and miRBase (version 21). The miRNA counts were aligned and quantified using the voom function in the limma package (v3.40.6) and normalized using the trimmed mean of M-values (TMM) function in the edgeR package (v3.26.8). miRNA expression was then converted to log<sub>2</sub> counts per million (log<sub>2</sub>CPM). The edgeR software package was used to assess differential miRNA expression. Pathway and Gene Ontology (GO) enrichment of the experimental miRNAs was performed using mirPath (v.3.0), which provided EASE scores and false discovery rates using Fisher's exact test and unbiased empirical distribution. Predicted interactions for the seven DEMs, the comprehensive list of predicted miRNA targets, as well as the GO and Kyoto Encyclopedia of Genes and Genomes (KEGG) enrichment analyses, are systematically presented in Additional file 3: Table S5, Additional file 4: Table S6, and Additional file 5: Table S7, respectively.

#### **Statistical analysis**

The identification criteria for DEMs between the SD and PD groups were  $P < 0.05$  and  $\text{abs}(\log_2\text{FC}) > \log_2(1.5)$  and  $\log_2(\text{AveExpr}) > 5$ . Ultimately, the predictive potential of seven DEMs was used for subsequent analyses (Additional file 1: Table S2–S3).

## **Results**

### **Clinical characteristics of patients with advanced NSCLC**

The clinical characteristics of the patients, including sex, smoking history, histology, initial treatment, drug, and efficacy assessment, are shown in Additional file 1: Table S1. In brief, 60% of the patients were male, and 40% had ever smoked (Additional file 1: Table S1). All patients had lung adenocarcinoma and were receiving anlotinib monotherapy. Eighty-five percent of patients received the initial anlotinib treatment as the third or fourth line. In addition, according to the drug evaluation, 14 patients had SD and 6 had PD (Additional file 1: Table S1).

**Representative imaging and pathological information**

We included representative pathology and CT images to further analyze the SD and PD subgroups. As one of the best antibody combinations for the diagnosis of lung adenocarcinoma, TTF-1 and napsin A were used for a staining analysis of samples from enrolled patients, and the results were positive (Fig. 1A). The immunohistochemical staining results for P40, a commonly used immunohistochemical marker for lung squamous cell carcinoma, were negative (Fig. 1A). Typical hematoxylin and eosin (HE) images from three patients are also shown in Fig. 1A. Patients were divided into the SD and PDs group according to changes in tumor size in response to anlotinib treatment. Figure 1B shows typical CT images for tumor size assessment at different time points after patients in the SD and PD groups received anlotinib. Moreover, the percentage of tumor size changes based on CT scan images are shown in Fig. 1C.

**Representative morphology and protein expression characteristics of plasma sEVs**

To confirm the presence of purified sEVs isolated from advanced NSCLC patients, we conducted NTA (Fig. 2A), TEM (Fig. 2B), and immunofluorescence imaging (Fig. 2C). Briefly, the diameters of the sEVs ranged from 30 to 150 nm (Fig. 2A). The

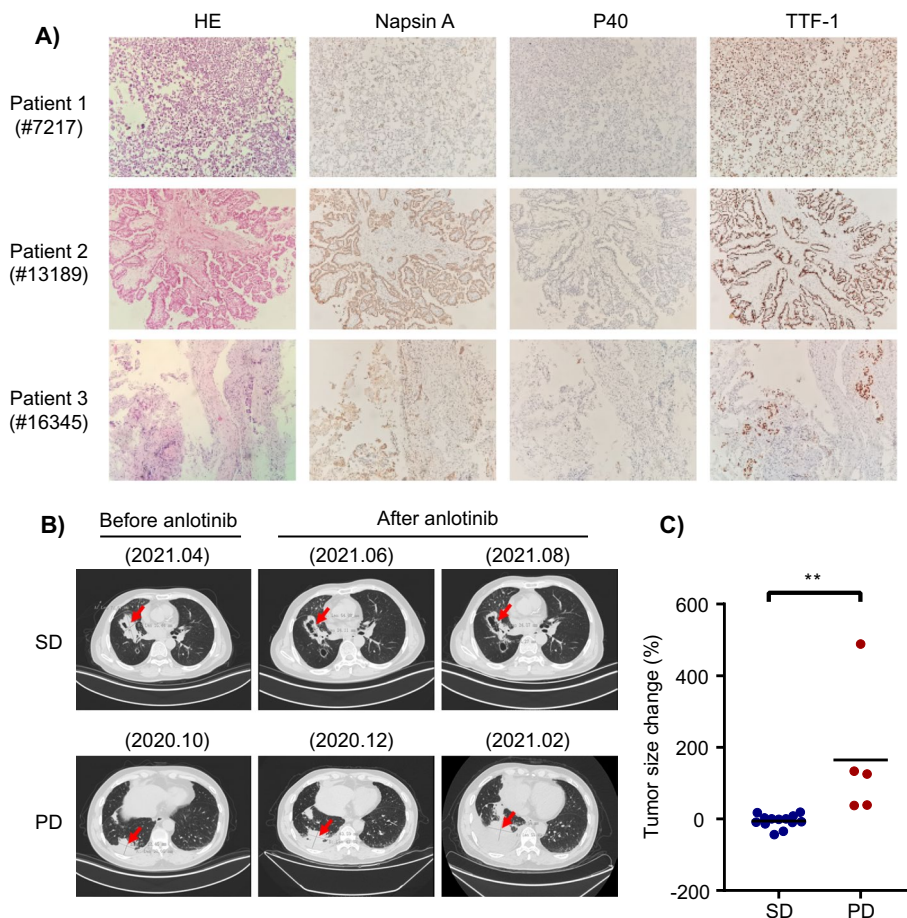


**Fig. 1** Representative imaging and pathological information. **A** Typical pathology images of HE and IHC staining. **B** Examples of CT images after treatment with anlotinib. **C** The percentage of tumor size changes in different groups

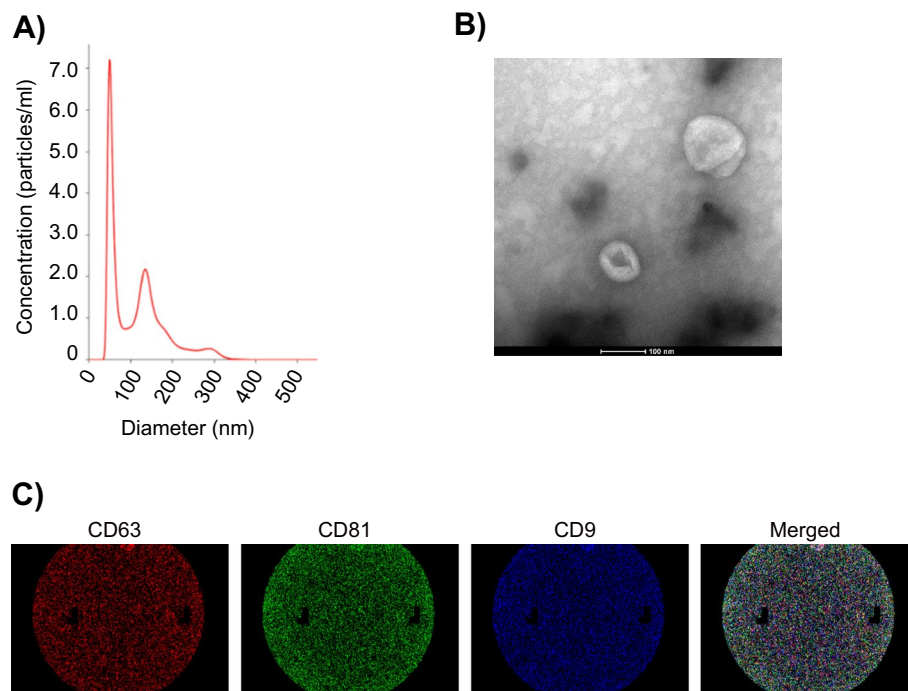


**Fig. 2** Representative morphological and protein expression features of plasma-derived sEVs. **A** Diameter distribution of sEVs according to the NTA analysis. **B** TEM images of sEVs. Scale bar, 100 nm. **C** Single-particle interferometric reflectance imaging analysis of the expression surface markers of plasma sEVs

morphology of the isolated sEVs was similar to a cup or bowl shape, as shown in Fig. 2B. In addition, the isolated sEVs were further characterized via immunophenotypic analysis using single-particle interferometric reflectance imaging staining for CD63, CD81, and CD9 (Fig. 2C).

#### Unsupervised clustering and differential expression of sEV miRNAs in SD and PD patients

Small RNA sequencing was performed to investigate the differential expression of miRNAs in sEVs from SD and PD patients. The bioinformatic data derived from the sEV miRNAs in plasma were normalized to obtain counts per million. The differences between SD and PD patients are clearly visualized in Additional file 1: Figure S3A. The differentially expressed sEV miRNAs identified in the preliminary screening are shown in Fig. 3A (Additional file 6: Table S10). Patients with advanced NSCLC in the PD group were differentiated from those in the SD group according to the sEV miRNA expression signature, as shown in Fig. 3A. To further focus on valuable DEMs, we set  $P < 0.05$  and  $\text{abs}(\log_2\text{FC}) > \log_2(1.5)$  and  $\log_2(\text{AveExpr}) > 5$  and finally focused on seven sEV miRNAs. The analysis results showed that miR-30a-3p, miR-150-5p, miR-122-5p, miR-10b-5p, miR-92a-3p, and miR-150-3p expression was significantly downregulated in the PD group (Fig. 3B–H, Additional file 1: Figure S3B). In addition, miR-941 expression was significantly upregulated in the PD group (Fig. 3D).

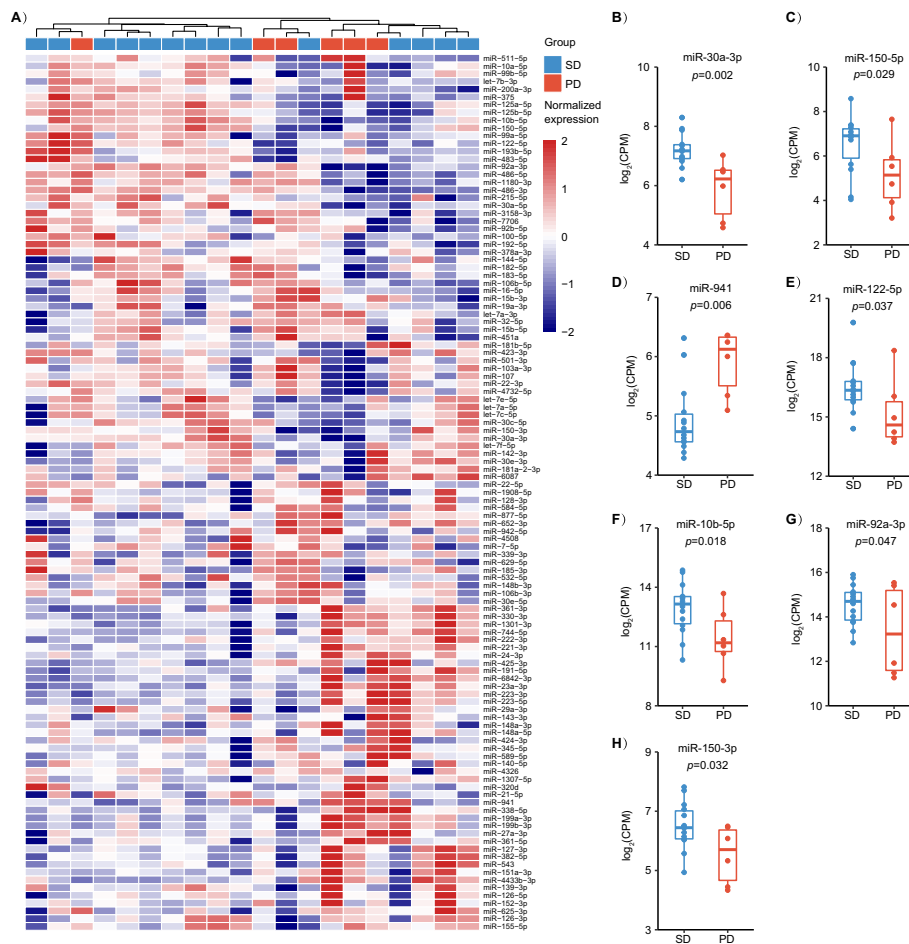


**Fig. 3** Unsupervised clustering and differential expression of sEV miRNAs in SD and PD patients. **A** Unsupervised hierarchical clustering of sEV miRNA profiles clearly separated into SD and PD samples. **B–H** Analysis of the miR-30a-3p, miR-150-5p, miR-941, miR-122-5p, miR-10b-5p, miR-92a-3p, and miR-150-3p levels in sEVs derived from SD and PD patients

**Unsupervised clustering and differential expression of sEV miRNAs in nonsmoking SD and PD patients**

To further verify the effect of clinical characteristics, such as smoking status, on the differential expression of miRNAs between the SD and PD groups, we further analyzed the data shown in Fig. 3. In nonsmoking patients, a heatmap showed that SD and PD could also be effectively distinguished according to the differential expression of sEV miRNAs (Additional file 1: Figure S4A, Fig. 4A, Additional file 7: Table S11). Furthermore, the seven DEMs showed the same change trend in nonsmoking patients (Fig. 4B–H). In comparison with the findings shown in Fig. 3, the discrepancies in the DEMs, including miR-150-5p, miR-941, miR-122-5p, miR-10b-5p, and miR-92a-3p, are more pronounced between the SD and PD groups in Fig. 4.

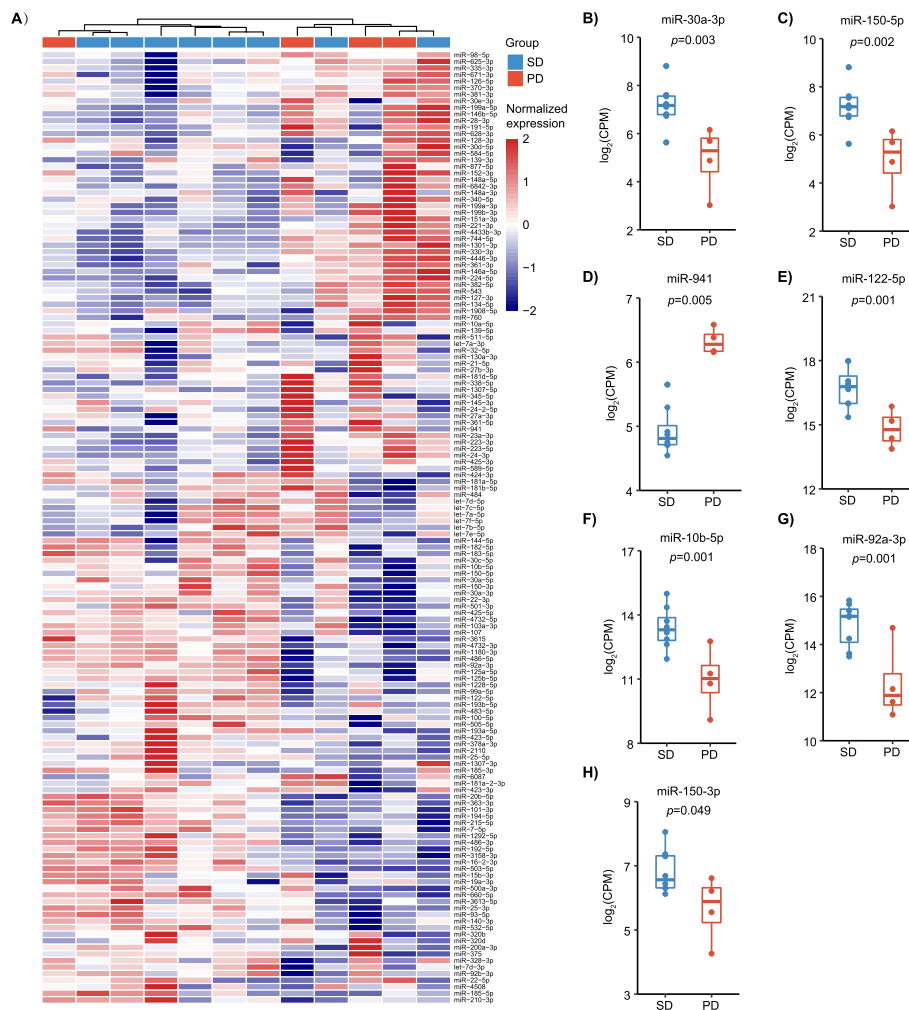


**Fig. 4** Unsupervised clustering and differential expression of sEV miRNAs in nonsmoking SD and PD patients. **A** Unsupervised hierarchical clustering of sEV miRNA profiles clearly separated into nonsmoking SD and PD samples. **B–H** Analysis of the miR-30a-3p, miR-150-5p, miR-941, miR-122-5p, miR-10b-5p, miR-92a-3p, and miR-150-3p levels in sEVs derived from nonsmoking SD and PD patients

**KEGG/GO analysis of the differentially expressed sEV miRNAs**

Bioinformatic analyses were then performed on the sEV miRNAs to identify molecular regulatory mechanisms. Analysis of differentially expressed sEV miRNAs between the PD and SD groups revealed the involvement of several cancer-related pathways identified in the KEGG database. Several signaling pathways in biological processes (Fig. 5A) were enriched according to an analysis of the KEGG database. These included processes such as biosynthesis, small molecule metabolism, and the immune system (Fig. 5A). Several pathways related to cellular components and molecular functions were also implicated according to the analysis of a bioinformatics miRNA target database (Fig. 5B). In addition, signaling pathways related to cellular processes, human diseases, environmental information processing, and genetic information processing were identified (Fig. 5C). The involvement of several cancer-related pathways, such as the TGF- $\beta$ , PI3K-Akt, MAPK, and p53 signaling pathways, highlights

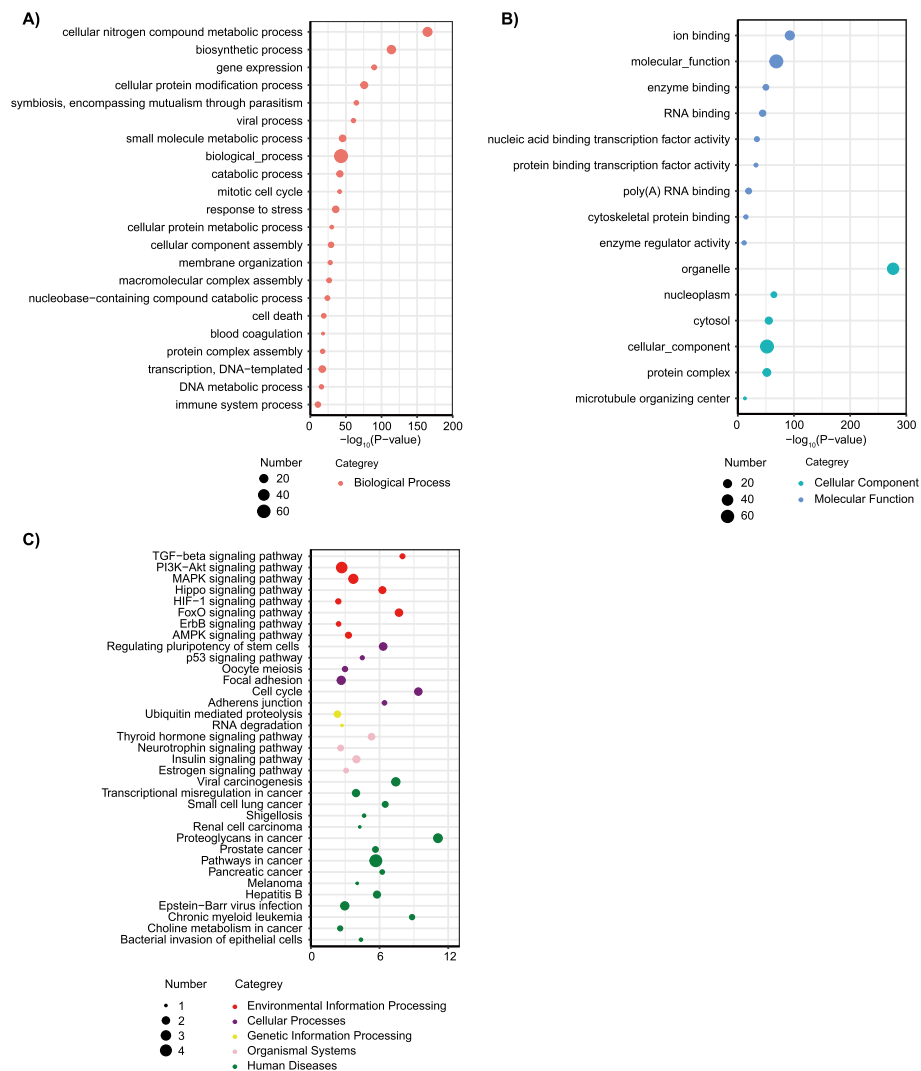


**Fig. 5** KEGG/GO analysis of the differentially expressed sEV miRNAs. **A** Bubble plot of enriched GOs (biological process terms) of the target genes of the DEMs between the SD and PD groups. **B** A bubble plot of enriched GOs (cellular component and molecular function) of the target genes of the DEMs between the SD and PD groups. **C** Bubble plot of enriched KEGG pathways of target genes of the DEMs between the SD and PD groups

the complex network of signaling events that contribute to cancer progression and response to therapy. For instance, the TGF- $\beta$  signaling pathway plays a dual role in cancer by acting as a tumor suppressor in the early stages and promoting metastasis in the later stages. As such, understanding how anlotinib modulates this pathway can provide insights into the drug’s therapeutic efficacy and potential resistance mechanisms.

Pathway analysis in lung adenocarcinoma patients treated with anlotinib is crucial for understanding the underlying molecular mechanisms and potential therapeutic targets. Anlotinib is a multitarget TKI that has shown efficacy in treating various cancers, including lung adenocarcinoma. By analyzing the differentially expressed sEV miRNAs, researchers can identify key pathways altered in response to anlotinib treatment. In

summary, pathway analysis provides a comprehensive view of the molecular alterations induced by anlotinib in lung adenocarcinoma. This information is invaluable for identifying potential biomarkers of treatment responses, understanding resistance mechanisms, and developing combination therapies to improve clinical outcomes.

## Discussion

Anlotinib is a novel multitarget TKI that has been widely used to treat advanced NSCLC (Huang et al. 2022). Several clinical trials have shown that anlotinib can significantly prolong the survival and progression-free survival rates of patients with advanced NSCLC and demonstrates good tolerability and safety (Jiang et al. 2022; Wang et al. 2023). As a result, anlotinib has become one of the main options for the second-line treatment of advanced NSCLC. However, the therapeutic effects of anlotinib vary from person to person, and not all patients may benefit from it. In addition, the adverse effects of anlotinib, such as hypertension, hypotension, bleeding, myocardial infarction, and abnormal liver and kidney function (Si et al. 2019), need to be considered. Therefore, before anlotinib is used, adequate assessment and preparation are required to ensure that patients can use the drug safely. However, there is currently a lack of liquid biopsy biomarkers for assessing the efficacy of anlotinib in treating patients with advanced NSCLC.

EVs can be released from cells and taken up by other tissues, carrying large amounts of genetic information (Dai et al. 2020). Many studies have shown that EVs have substantial potential in tumor diagnosis and therapeutic efficacy assessment (Tan et al. 2023). In tumor treatment, drug efficacy can be assessed by analyzing microRNA levels in sEVs produced by tumor cells (Mao et al. 2023). In addition, the detection of sEVs in blood or other body fluids can be an effective tool for early diagnosis, as they can appear in the body's circulation at an early stage of tumor development and growth (Wang et al. 2021). Thus, investigating sEVs will undoubtedly provide us with more valuable information to improve the prevention and treatment of tumors. Therefore, in this study, we explored the potential of EV miRNAs as biomarkers to evaluate the efficacy of anlotinib treatment in advanced NSCLC patients. To the best of our knowledge, this is the first report focusing on plasma sEV miRNAs as biomarkers for evaluating the efficacy of anlotinib.

In this study, we identified seven sEV miRNAs (miR-30a-3p, miR-150-5p, miR-941, miR-122-5p, miR-10b-5p, miR-92a-3p, and miR-150-3p) that exhibited significant differences in expression between NSCLC patients with SD and PD. Our results showed that high miR-941 expression was correlated with poor response to anlotinib. Patients with low expression of miR-30a-3p, miR-150-5p, miR-122-5p, miR-10b-5p, miR-92a-3p, and miR-150-3p may respond better to anlotinib treatment. Therefore, sEV miRNAs show substantial potential for evaluating the efficacy of anlotinib for treating advanced NSCLC patients.

Previous studies have shown the role of miR-30a-3p in treating arteriosclerosis obliterans (Zhang et al. 2023a). Conrad et al. reported that high expression of miR-30a-3p is associated with improved prognosis in HNSCC patients (Conrad et al. 2023). Niemira et al. investigated the potential of miR-150-5p as a prognostic marker for high-grade serous ovarian cancer (Niemira et al. 2023). miR-150-5p also showed good promise in prostate cancer diagnostics (Cruz-Burgos et al. 2023). Surapaneni et al. reported that the proliferation of breast cancer cells is regulated by miR-941 (Surapaneni et al. 2020).

miR-941 may function as an oncogenic biomarker in laryngeal squamous cell carcinoma (Zhao et al. 2020). miR-122-5p plays a role in inducing apoptosis and inhibiting pancreatic cancer cell growth by targeting ASCT2 (Ren et al. 2023). Tao et al. reported that miR-122-5p may be associated with the regulation of the metastasis and invasion of intrahepatic cholangiocarcinoma (Tao et al. 2023). In glioblastoma, Du et al. reported that PD-L1-driven immune evasion is regulated by the miR-10b-5p-mediated regression of TET2 (Du et al. 2023). The role of miR-10b-5p as a target for mediating sarcoma progression has also been reported (Yoshida et al. 2023). Dai et al. reported that miR-92a-3p could be a prognostic biomarker for lung adenocarcinoma (Dai et al. 2023). In patients with metastatic colorectal cancer, high miR-92a-3p expression is associated with a poor prognosis (Gherman et al. 2023). In 2023, Li et al. reported that colon cancer growth is promoted by the miR-150-3p/SRCIN1/Wnt axis (Li et al. 2023b). In lung squamous cell carcinoma, miR-150-3p may be a critical oncogenic target in regulating the malignant phenotype (Mizuno et al. 2021). However, this study is the first to report the regulatory relationship between these seven miRNAs and anlotinib.

This study had some limitations. First, future research into regulatory mechanisms should consider the need for validation by *in vitro* cell experiments and *in vivo* animal experiments. Second, further patient recruitment is required for prospective clinical validation with a larger sample size before implementing the model in clinical practice. Third, we identified only seven plasma sEVmiRNAs as the most promising biomarkers for identifying patients who would benefit from anlotinib, and other sEVmiRNAs need to be tested.

## Conclusions

In this study, we investigated the ability of plasma sEV miRNAs to serve as biomarkers to identify true responders to anlotinib. After comprehensively examining sEV miRNA expression in advanced NSCLC patients treated with anlotinib, we identified seven differentially expressed sEV miRNAs. Interestingly, all of these small extracellular miRNAs showed an excellent ability to identify true responders. The different biological pathways involved in this process were analyzed. The results suggested that plasma sEV miRNAs had potential as noninvasive biomarkers for identifying true responders to anlotinib.

## Abbreviations

NSCLC	Non-small cell lung cancer
sEV	Small extracellular vesicle
miRNA	MicroRNA
SD	Stable disease
PD	Progressive disease
DEMs	Differentially expressed miRNAs
TKI	Tyrosine kinase inhibitor
CT	Computed tomography
NTA	Nanoparticle tracking analysis
TEM	Transmission electron microscopy
lincRNAs	Long intergenic noncoding RNAs
rRNAs	Ribosomal RNAs
TMM	Trimmed mean of M-values
log <sub>2</sub> CPM	Log <sub>2</sub> counts per million
GO	Gene Ontology
KEGG	Kyoto Encyclopedia of Genes and Genomes
HE	Hematoxylin and eosin

## Supplementary Information

The online version contains supplementary material available at <https://doi.org/10.1186/s12645-024-00273-3>.

Additional file 1.  
Additional file 2.  
Additional file 3.  
Additional file 4.  
Additional file 5.  
Additional file 6.  
Additional file 7.

### Acknowledgements

All of the authors would like to thank the patients and their families for their support.

### Author contributions

Conceptualization: W.-W.M., G.-A.Q., H.-B.H., and Z.-D.D.; Methodology: H.-A.M., Z.-F.C., Z.-J.Y., X.-X.Y., L.-Z.K., C. S., and N.-B.N.; Investigation: H.-A.M., Z.-F.C., Z.-J.Y., X.-X.Y., L.-Z.K., C. S., and N.-B.N.; Visualization: Z.-F.C., Z.-J.Y., and H.-A.M.; Funding acquisition: W.-W.M., G.-A.Q., H.-B.H.; Project administration: W.-W.M., G.-A.Q., H.-B.H., Z.-D.D., and Z.-F.C.; Supervision: W.-W.M., G.-A.Q., H.-B.H. and Z.-D.D.; Writing, original draft: Z.-F.C., H.-A.M., and Z.-J.Y.; Writing, review & editing: W.-W.M., G.-A.Q., H.-B.H. and Z.-D.D.

### Funding

This study was supported by the Beijing Kangmeng Science Foundation (No. YWJKJHKYJJ-F2236E) and the Efficacy and Correlation of Arotinib in the Treatment of Advanced Small Cell Lung Cancer (No. TB207006).

### Availability of data and materials

The datasets used and/or analyzed during the current study are available from the corresponding author upon reasonable request.

### Declarations

#### Competing interests

Z.-F.C., Z.-J.Y., X.-X.Y., L.-Z.K., C.S., N.-B.N., and Z.-D.D. are affiliated with 3D Medicines Inc. and are current or former employees. The authors have no other potential competing interests to disclose.

Received: 2 April 2024 Accepted: 19 June 2024

Published online: 02 July 2024

### References

- Conrad O, Burgy M, Foppolo S, Jehl A, Thiery A, Guihard S, Vauchelles R, Jung AC, Mourtada J, Macabre C et al (2023) Tumor-suppressive and immunomodulating activity of miR-30a-3p and miR-30e-3p in HNSCC cells and tumoroids. *Int J Mol Sci*. <https://doi.org/10.3390/ijms241311178>
- Cruz-Burgos M, Cortes-Ramirez SA, Losada-Garcia A, Morales-Pacheco M, Martinez-Martinez E, Morales-Montor JG, Servin-Haddad A, Izquierdo-Luna JS, Rodriguez-Martinez G, Ramos-Godinez MDP et al (2023) Unraveling the role of EV-Derived miR-150-5p in prostate cancer metastasis and its association with high-grade gleason scores: implications for diagnosis. *Cancers*. <https://doi.org/10.3390/cancers15164148>
- Dai J, Su Y, Zhong S, Cong L, Liu B, Yang J, Tao Y, He Z, Chen C, Jiang Y (2020) Exosomes: key players in cancer and potential therapeutic strategy. *Signal Transduct Target Ther* 5:145. <https://doi.org/10.1038/s41392-020-00261-0>
- Dai H, Li L, Yang Y, Chen H, Dong X, Mao Y, Gao Y (2023) Screening microRNAs as potential prognostic biomarkers for lung adenocarcinoma. *Ann Med* 55:2241013. <https://doi.org/10.1080/07853890.2023.2241013>
- Du W, Chen D, Wei K, Yu D, Gan Z, Xu G, Yao G (2023) MiR-10b-5p impairs TET2-mediated inhibition of PD-L1 transcription thus promoting immune evasion and tumor progression in glioblastoma. *Tohoku J Exp Med* 260:205–214. <https://doi.org/10.1620/tjem.2023.J028>
- Gherman A, Balacescu L, Popa C, Cainap C, Vlad C, Cainap SS, Balacescu O (2023) Baseline expression of exosomal miR-92a-3p and miR-221-3p could predict the response to first-line chemotherapy and survival in metastatic colorectal cancer. *Int J Mol Sci*. <https://doi.org/10.3390/ijms241310622>
- Guo S, Qin H, Liu K, Wang H, Bai S, Liu S, Shao Z, Zhang Y, Song B, Xu X et al (2021) Blood small extracellular vesicles derived miRNAs to differentiate pancreatic ductal adenocarcinoma from chronic pancreatitis. *Clin Transl Med* 11:e520. <https://doi.org/10.1002/ctm2.520>
- Huang A, Wang W, Qin R, Chen G, Gu A, Han B (2022) Efficacy, safety, and prognostic factors of anlotinib treatment in advanced non-small cell lung cancer patients. *J Cancer Res Ther* 18:1299–1305. [https://doi.org/10.4103/jcrt.jcrt\\_835\\_21](https://doi.org/10.4103/jcrt.jcrt_835_21)

- Jiang F, Li J, Kong X, Sun P, Qu H (2022) Efficacy and safety evaluations of anlotinib in patients with advanced non-small cell lung cancer treated with bevacizumab. *Front Pharmacol* 13:973448. <https://doi.org/10.3389/fphar.2022.973448>
- Kong F, Wang Z, Wang N, Zhang D, Liao D, Zhang J, Sun Y, Zhang H, Jia Y (2023) Maintenance anlotinib improves the survival prognosis of extensive-stage small cell lung cancer: a single-arm, prospective, phase II study. *Am J Cancer Res* 13:3679–3685
- Li P, Bai Y, Shan B, Zhang W, Liu Z, Zhu Y, Xu X, Chen Q, Sheng X, Deng X et al (2021) Exploration of potential diagnostic value of protein content in serum small extracellular vesicles for early-stage epithelial ovarian carcinoma. *Front Oncol* 11:707658. <https://doi.org/10.3389/fonc.2021.707658>
- Li L, Zhang F, Zhang J, Shi X, Wu H, Chao X, Ma S, Lang J, Wu M, Zhang D, Liang Z (2023a) Identifying serum small extracellular vesicle microRNA as a noninvasive diagnostic and prognostic biomarker for ovarian cancer. *ACS Nano* 17:19197–19210. <https://doi.org/10.1021/acsnano.3c05694>
- Li S, Han W, He Q, Wang Y, Jin G, Zhang Y (2023b) Ginsenoside Rh2 suppresses colon cancer growth by targeting the miR-150-3p/SRCIN1/Wnt axis. *Acta Biochim Biophys Sin* 55:633–648. <https://doi.org/10.3724/abbs.2023032>
- Mao Y, Zhang M, Wang L, Lu Y, Hu X, Chen Z (2023) Role of microRNA carried by small extracellular vesicles in urological tumors. *Front Cell Dev Biol* 11:1192937. <https://doi.org/10.3389/fcell.2023.1192937>
- Mizuno K, Tanigawa K, Misono S, Suetsugu T, Sanada H, Uchida A, Kawano M, Machida K, Asai S, Moriya S et al (2021) Regulation of oncogenic targets by tumor-suppressive miR-150–3p in lung squamous cell carcinoma. *Biomedicines*. <https://doi.org/10.3390/biomedicines9121883>
- Niemira M, Erol A, Bielska A, Zeller A, Skwarska A, Chwialkowska K, Kuzmicki M, Szamatowicz J, Reszec J, Knapp P et al (2023) Identification of serum miR-1246 and miR-150-5p as novel diagnostic biomarkers for high-grade serous ovarian cancer. *Sci Rep* 13:19287. <https://doi.org/10.1038/s41598-023-45317-7>
- Ren P, Wu NA, Fu S, Wang W, Li QI, Cheng Q (2023) miR-122–5p restrains pancreatic cancer cell growth and causes apoptosis by negatively regulating ASCT2. *Anticancer Res* 43:4379–4388. <https://doi.org/10.2187/anticancer.16634>
- Shen G, Zheng F, Ren D, Du F, Dong Q, Wang Z, Zhao F, Ahmad R, Zhao J (2018) Anlotinib: a novel multi-targeting tyrosine kinase inhibitor in clinical development. *J Hematol Oncol* 11:120. <https://doi.org/10.1186/s13045-018-0664-7>
- Si X, Zhang L, Wang H, Zhang X, Wang M, Han B, Li K, Wang Q, Shi J, Wang Z et al (2019) Management of anlotinib-related adverse events in patients with advanced non-small cell lung cancer: experiences in ALTER-0303. *Thoracic Cancer* 10:551–556. <https://doi.org/10.1111/1759-7714.12977>
- Surapaneni SK, Bhat ZR, Tikoo K (2020) MicroRNA-941 regulates the proliferation of breast cancer cells by altering histone H3 Ser 10 phosphorylation. *Sci Rep* 10:17954. <https://doi.org/10.1038/s41598-020-74847-7>
- Tan M, Ge Y, Wang X, Wang Y, Liu Y, He F, Teng H (2023) Extracellular vesicles (EVs) in tumor diagnosis and therapy. *Technol Cancer Res Treat* 22:15330338231171464. <https://doi.org/10.1177/15330338231171463>
- Tao L, Wang Y, Shen Z, Cai J, Zheng J, Xia S, Lin Z, Wan Z, Qi H, Jin R et al (2023) Activation of IGF1R4 via unconventional mechanism of miRNA attenuates metastasis of intrahepatic cholangiocarcinoma. *Hep Intl*. <https://doi.org/10.1007/s12072-023-10552-7>
- Wang Y, Zhao R, Jiao X, Wu L, Wei Y, Shi F, Zhong J, Xiong L (2021) Small extracellular vesicles: functions and potential clinical applications as cancer biomarkers. *Life*. <https://doi.org/10.3390/life11101044>
- Wang M, Zhao J, Chen T, Hu X, Wang L, Shi Y, Liu Y (2023) Efficacy and safety of osimertinib plus anlotinib in advanced non-small-cell lung cancer patients after drug resistance. *Thoracic Cancer* 14:873–880. <https://doi.org/10.1111/1759-7714.14819>
- Yoshida K, Yokoi A, Kitagawa M, Sugiyama M, Yamamoto T, Nakayama J, Yoshida H, Kato T, Kajiyama H, Yamamoto Y (2023) Downregulation of miR-10b-5p facilitates the proliferation of uterine leiomyosarcoma cells: a microRNA sequencing-based approach. *Oncol Rep*. <https://doi.org/10.3892/or.2023.8523>
- Zhang K, Ma X, Gao H, Wang H, Qin H, Yang S, Liu X (2020) Efficacy and safety of anlotinib in advanced non-small cell lung cancer: a real-world study. *Cancer Manag Res* 12:3409–3417. <https://doi.org/10.2147/CMAR.S246000>
- Zhang M, Chen Y, Niu F, Luo X, Li J, Hu W (2023a) MicroRNA-30a-3p: a potential noncoding RNA target for the treatment of arteriosclerosis obliterans. *Aging*. <https://doi.org/10.1863/aging.205154>
- Zhang Y, Zhao L, Li Y, Wan S, Yuan Z, Zu G, Peng F, Ding X (2023b) Advanced extracellular vesicle bioinformatic nano-materials: from enrichment, decoding to clinical diagnostics. *J Nanobiotechnol* 21:366. <https://doi.org/10.1186/s12951-023-02127-3>
- Zhao Q, Zheng X, Guo H, Xue X, Zhang Y, Niu M, Cui J, Liu H, Luo H, Yang D et al (2020) Serum exosomal miR-941 as a promising oncogenic biomarker for laryngeal squamous cell carcinoma. *J Cancer* 11:5329–5344. <https://doi.org/10.7150/jca.45394>
- Zheng D, Zhu Y, Zhang J, Zhang W, Wang H, Chen H, Wu C, Ni J, Xu X, Nian B et al (2022) Identification and evaluation of circulating small extracellular vesicle microRNAs as diagnostic biomarkers for patients with indeterminate pulmonary nodules. *J Nanobiotechnol* 20:172. <https://doi.org/10.1186/s12951-022-01366-0>
- Zhu Q, Ni R, Guan X (2023) Cost-effectiveness analysis of anlotinib as a third-line or further treatment for advanced non-small cell lung cancer in China. *Transl Lung Cancer Res* 12:1782–1789. <https://doi.org/10.2103/tlcr-23-456>

## Publisher's Note

Springer Nature remains neutral with regard to jurisdictional claims in published maps and institutional affiliations.